Supporting Information

Ropars et al. 10.1073/pnas.1100758108

SI Text

Production of Full-Length Proteins. Sequences coding for full-length (FL) XRCC4$^{1–336}$ and Cernunnos$^{1–299}$ were cloned in pETM13-LIC vector. The cloning leads to an additional MAGAAS sequence at the N terminus and a six histidine tag at the C terminus of each protein. Production in *Escherichia coli* Rosetta strain was conducted as already described (1) excepted that the cells were resuspended in buffer Tris-HCl 20 mM pH 8, EDTA 5 mM, KCl 100 mM, 2-Mercaptoethanol 10 mM, saccharose 20%, Lysozyme 1 mg/mL, Benzamidine 34 μg/l, PMSF 0,1 mM. After sonication and clarification, a 5 ml HiTrap Q column was loaded with the cells extract, washed with the buffer A (Tris-HCl 20 mM pH 8, EDTA 2 mM, glycerol 10%, 2-Mercaptoethanol 10 mM, Benzidine 34 μg/l). The $X4^{FL}$ and Cernunnos^{FL} proteins were eluted with a linear gradient of buffer B (buffer A + 0,5M NaCl). Enriched fractions were dialyzed against buffer C (Tris-Cl 20 mM pH 8, KCl 100 mM, glycerol 10%, 2-Mercaptoethanol 10 mM, Benzamidine 34 μg/l), loaded on a NiNTA column, washed with the buffer C, then with the buffer C±20mM Imidazole. Finally the full lengh proteins were eluted with the buffer C±300 mM Imidazole.

The purity of the purified proteins was estimated by SDS/PAGE gels (Fig. S1). The integrity of the full-length proteins was confirmed by N-terminal sequencing and detection of the C-terminal histidine tag with Western blot. The overall structural integrity of the full-length proteins was evaluated by analytical size exclusion chromatography (Fig. S1*B*)

Production of Seleno-Methionine Cernunnos$^{1–224}$. Production of Cernunnos$^{1–224}$ labeled with seleno-methionine was performed with the same protocol, except that the cellular cultures were performed in minimal medium supplemented with most amino acids and seleno-methionine as detailed here. For 2 liters medium, the following solutions are prepared: (*i*) amino acids solutions: 17 solutions with 400 mg of 17 amino acids (Sigma Aldrich) prepared separately are dissolved in 40 mL sterilized H_2O (17 amino acids are all amino acids except methionine, tyrosine, and cysteine); (*ii*) seleno-methionine solution: 250 mg of seleno-methionine (Acros Organic) are dissolved in 200 ml sterilized H_2O; (*iii*) salt solution: a solution with 4 g KH_2PO_4, 16 g $NaHPO_4$, 1 g NaCl dissolved in 1,100 mL; (*iv*) stock oligo solution: prepared with 0.5 g EDTA, 415 mg $FeClA_3$, 42 mg $ZnCl_2$, 6.5 mg $CuClA_2.2H_2O$, 5 mg $CoCl_2.6H_2O$, 5 mg H_3BO_3 dissolved in 500 mL H_2O and filtered on 0.22-μm filter.

The medium is prepared by mixing the salt solution (*iii*), 20 ml of stock oligo solution (*iv*), 2 ml of thiamine at 1 mg/mL, 2 mL of biotine at 1mg/mL. We add 0.49 g $MgSO_4$ and 0.1 g $CaCl_2$ and heat a little at 37 °C if necessary. We add 4 g glucose and 1 g $(NH4)_2SO_4$ and 2 ml glycerol 50%. This intermediate solution is filtered on 0.22 μm filter. We finally add the 17 solutions of amino acids (*i*) and the solution of seleno-methionine (*ii*) and the antibiotic required.

Refinement of the X4–Cernunnos Interface with Rosetta Modeling. The modeling was under the constraint of the electron density map with the low-resolution density map fitting protocol developed in the Rosetta 3.1 program (2). Two hundred models were generated using as options relax:fast, relax:fastrelax_repeats 4, relax:jump_move true, edensity:mapreso 5.0, edensity:grid_spacing 2.0, edensity:realign min, edensity:sliding_window_wt 0.2, edensity:sliding_window 5, ex1, ex2aro, and the score13_env_hb scoring weights. The most likely atomic arrangement at the X4–Cernunnos interface was selected by scoring these models using the docking_local_refine option of the docking module in Rosetta2.3, which allows for a short minimization of the interface before scoring with ex1, ex2aro_only, and score12 options (3).

1. Malivert L, et al. (2010) Delineation of the Xrcc4-interacting region in the globular head domain of cernunnos/XLF. *J Biol Chem* 285:26475–26483.
2. DiMaio F, Tyka MD, Baker ML, Chiu W, Baker D (2009) Refinement of protein structures into low-resolution density maps using Rosetta. *J Mol Biol* 392:181–190.
3. Gray JJ, et al. (2003) Protein-protein docking with simultaneous optimization of rigid-body displacement and side-chain conformations. *J Mol Biol* 331:281–299.

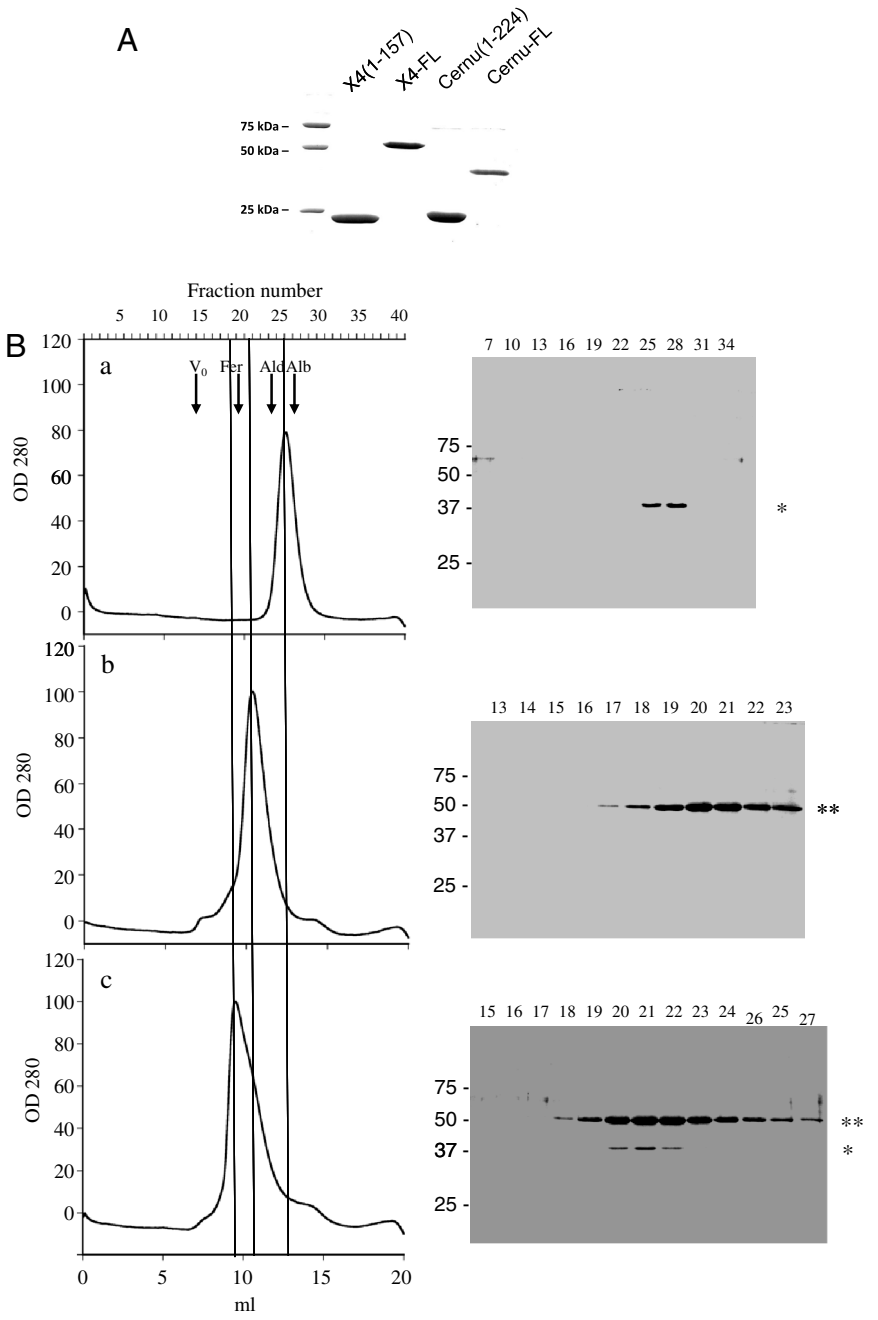
A
X4(1-157)
X4-FL
Cernu(1-224)
Cernu-FL
75 kDa –
50 kDa –
25 kDa –
B
Fraction number
a
b
c
V_0
Fer
Ald
Alb
OD 280
ml
*
**
**
*

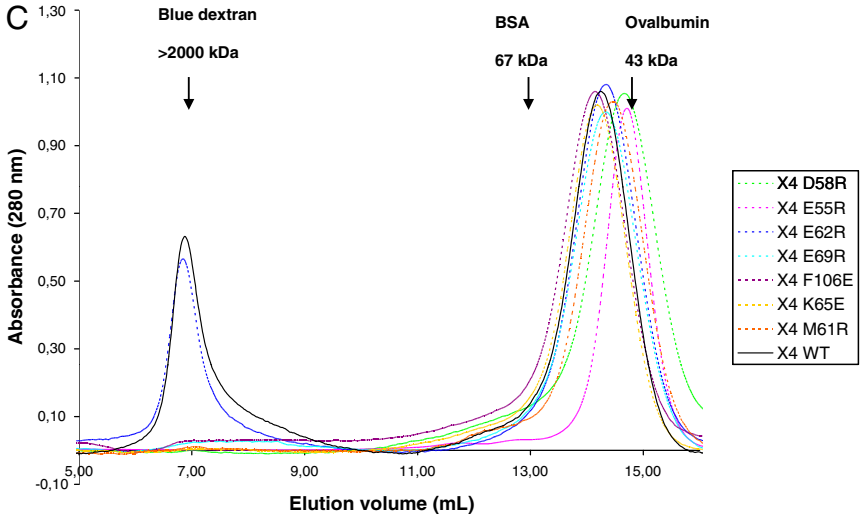

Fig. S1. (*A*) Analysis by SDS/PAGE gels of the X4 and Cernunnos wild-type proteins used in this study. X4 and Cernunnos lanes correspond to the truncated $X4^{1–157}$ and $Cernunnos^{1–224}$ proteins with MW of 21.5 kDa and 26.7 kDa, respectively. The X4 and Cernunnos full-length proteins correspond to $X4^{1–336}$ and $Cernunnos^{1–299}$ with MW of 39.5 kDa and 34.6k Da. respectively. All proteins are purified with a 6-His C-terminal tag. SDS/PAGE gels were carried out with representative fractions for each mutant after size exclusion chromatography. The proteins were analyzed by Western blot with an anti-6His antibody. $X4^{FL}$ migrates at higher MW (approximately 50 kDa) as already reported (1) DNA repair). Trace amounts of a higher MW contaminant (approximately 75 kDa) are observed in Cernunnos samples. Trypsin digestion and mass spectrometry analysis identified this contaminant as *E. coli* bifunctional polymyxin resistance protein ArnA. (*B*) Characterization of the interaction between CernunnosFL and XRCC4FL by SEC. Left panels: Chromatograms of proteins injected on Superdex S200 10/300GL (GE Healthcare, Vtot = 24 ml). Volume of elution of the standards are indicated: V_0 = dextran blue; Fer = Ferritin (440 kD); Ald = Aldolase (158 kD); Alb = Albumine (67 kD). (A) Cernunnos (6 nmoles). (B) XRCC4 (15 nmoles). (C) 15 nmoles of XRCC4 + 3 nmoles of Cernunnos after 15 min incubation at RT. Right panels: SDS/PAGE of fractions of the chromatogram shown on the left. (*) Full-length Cernunnos. (**) Full-length XRCC4. (*C*) SEC analyses of X4 proteins (WT and variants) used in this study. SEC analyses of wild-type X4 (black), and mutants were obtained by injecting 100 μl samples at 50 μM concentration on a Superdex-200 10/30 (GE Healthcare). Experiments were realized in 25 mM sodium phosphate pH 8.0, 150 mM NaCl and 10 mM β-mercaptoethanol. Some aggregates, which elute in the void volume of the column, are observed for X4 WT and X4 variant E62R.

1 Recuero-Checa, et al. (2009) Electron microscopy of Xrcc4 and the DNA ligase IV–Xrcc4 DNA repair complex. *DNA Repair (Amst)* 392:181–190.

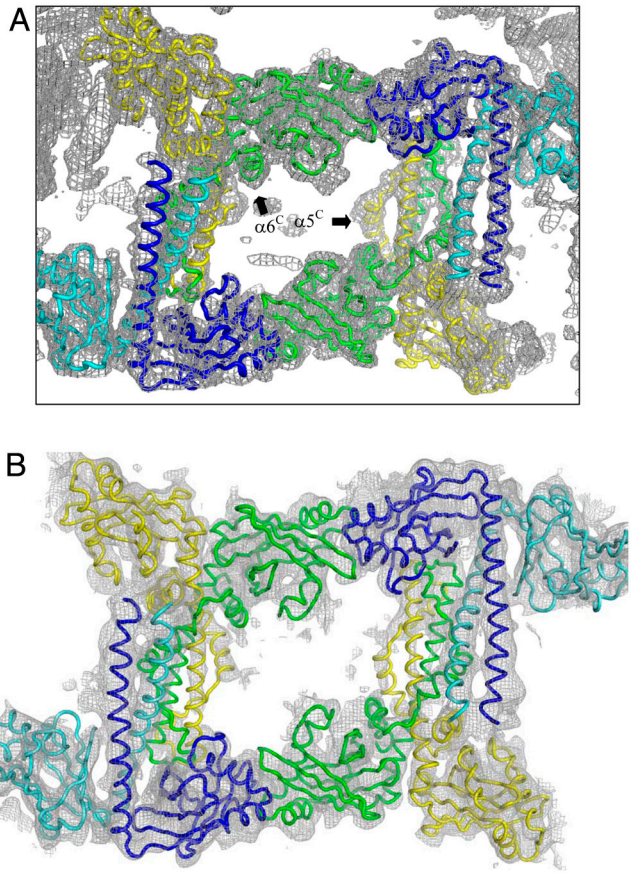
A
α6c
α5c
B

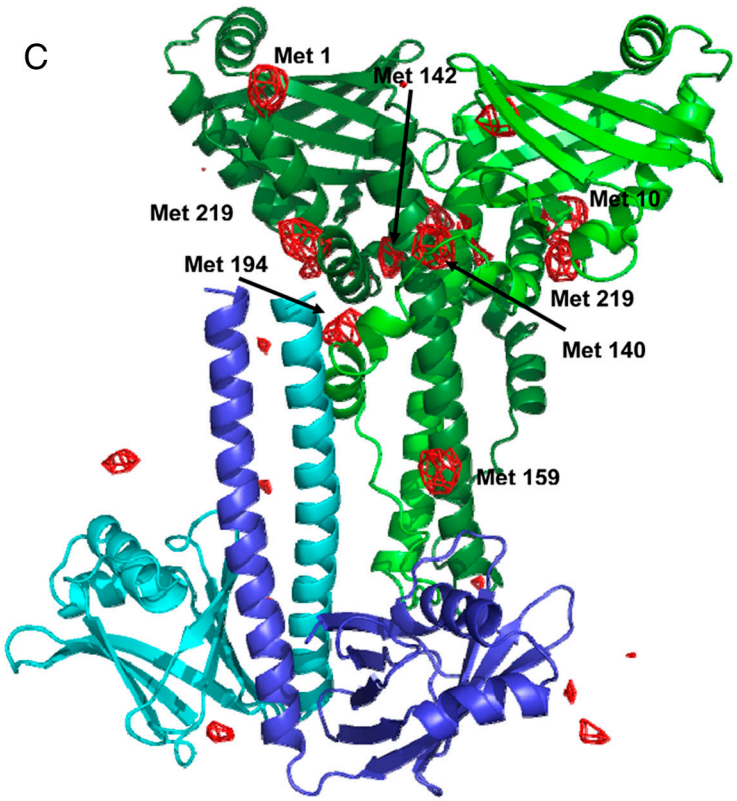
C
Met 1
Met 142
Met 219
Met 10
Met 194
Met 219
Met 140
Met 159

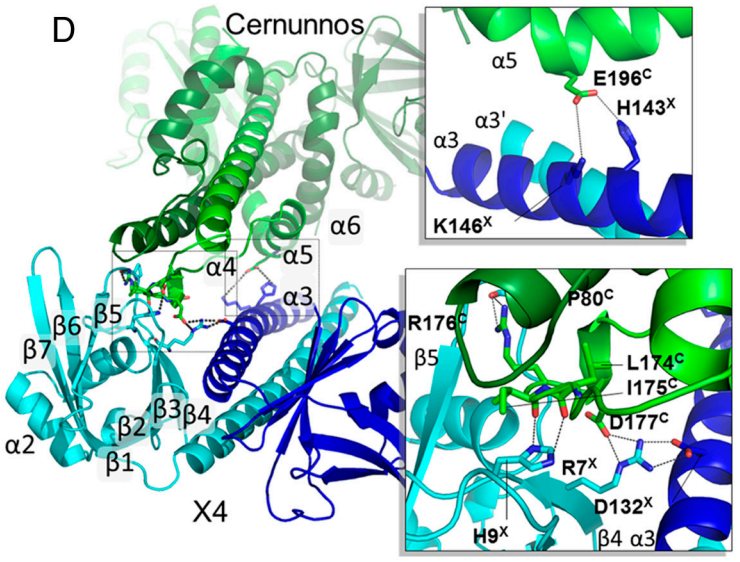
D
Cernunnos
α5
E196C
H143X
α3'
α3
K146X
α6
α4
α5
α3
β6
β5
β7
β3
β4
β2
α2
β1
X4
P80C
R176C
β5
L174C
I175C
D177C
R7X
D132X
H9X
β4 α3

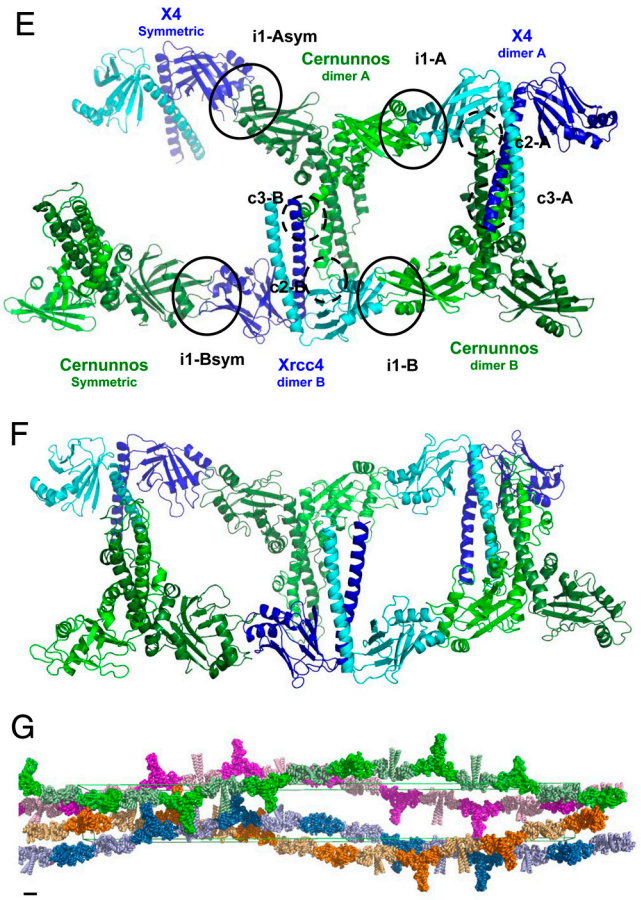

Fig. S2. (*A*) Electron density maps of the X4–Cernunnos complex at 5.5 Å. The X4 homodimer is colored in dark and light blue and the Cernunnos homodimer is colored in green and yellow. Representation of the sigma weighted $2F_o$-F_c electron density map from final refinement on two X4–Cernunnos complexes present in the asymmetric unit. The map shown in gray mesh is contoured at 1.0σ level. Positions of the Cernunnos helices α5 and α6 of are indicated by black arrow. The clear electron density maps on these helices contributed, in addition to seleno-methionine data, to identify the respective positions of X4 and Cernunnos molecules. X4 and Cernunos chains were clearly defined except for the Cernunnos regions of 170–173 and 178–184 and the X4 regions of 1–10 and 78–84 for which we observed weak electron density. (*B*) Composite annealed omit electron density map superimposed on the two X4–Cernunnos complexes present in the asymmetric unit. The color coding and orientation are the same as in *A*, and the map is contoured at 2.0 sigma level. (*C*) Electron density maps obtained with the (SeMet)Cernunnos protein. The color coding is the same as in *A*. Eight out of nine SeMet Cernunnos were visible in the Fourier anomalous difference maps with data collected at Se edge. The map shown in red mesh is contoured at 3.0 σ level. We identified eight out of nine Cernunnos methionine. The last methionine is at position 212, and its side chain was shown to adopt alternate positions in the structure of Cernunnos alone (1). (*D*) Molecular modelling of contact region "c2" with Rosetta software and electron density maps constraints. To model the likely contacts occurring at the c2 interface, we applied the same protocol as the one used to model the "i1" interface. From the best energy model, the c2 interface appears rather weak with less than 10 contacts (less than five residues in each partner) distributed over two small interacting patches. The first patch might be stabilized by a long range electrostatic interaction between $E196^C$ from Cernunnos (α5) and both $K146^X$ and $H143^X$ from XRCC4 (α3). The other interacting patch is first composed of a salt bridge between $R7^X$, $D132^C$ and $D177^C$ and a small hydrogen-bond network between $H9^X$ side chain and the backbone carbonyls of both $I175^C$ and $L174^C$ residues. There might be an additional hydrogen-bond between $R176^C$ and $P80^X$ backbone carbonyl. (*E*) Repetition of the X4–Cernunnos interface through crystal symmetry element 6_5. Same view as in Fig. 1*A*. The interfaces i1-A and i1-B observed within the asymmetric unit between head domains are repeated when applying crystal symmetry 6_5 of the crystal. For clarity, only two such additional symmetric interfaces have been represented (named i1-Asym and i1-Bsym). (*F*) Repetition of the X4–Cernunnos interface through crystal symmetry element 6_4 in SeMet crystals. Same view as in Fig. S4*B*. The interfaces i1-A and i1-B observed within the asymmetric unit between head domains are repeated when applying crystal symmetry 6_4 of the crystal. The filament in the top of the figure superimposes well with the one observed in the top of Fig. S4*B*. The second filament, in the bottom, presents a different orientation in spacegroup $P6_422$ compared to the one observed in spacegroup $P6_522$ in the bottom of Fig. 4*B*. (*G*) The packing of Cernunnos–X4 filaments in the crystal form $P6_522$. The unit cell is represented in green. The figure presents the parallel packing of four filaments along one unit cell with X4 in light colors and Cernunnos in dark colors along the symmetry axis 6_5. Bars represent 2 nm.

1 Li Y, et al. (2008) Crystal structure of human XLF/Cernunnos reveals unexpected differences from XRCC4 with implications for NHEJ. *EMBO J* 27:290–300.

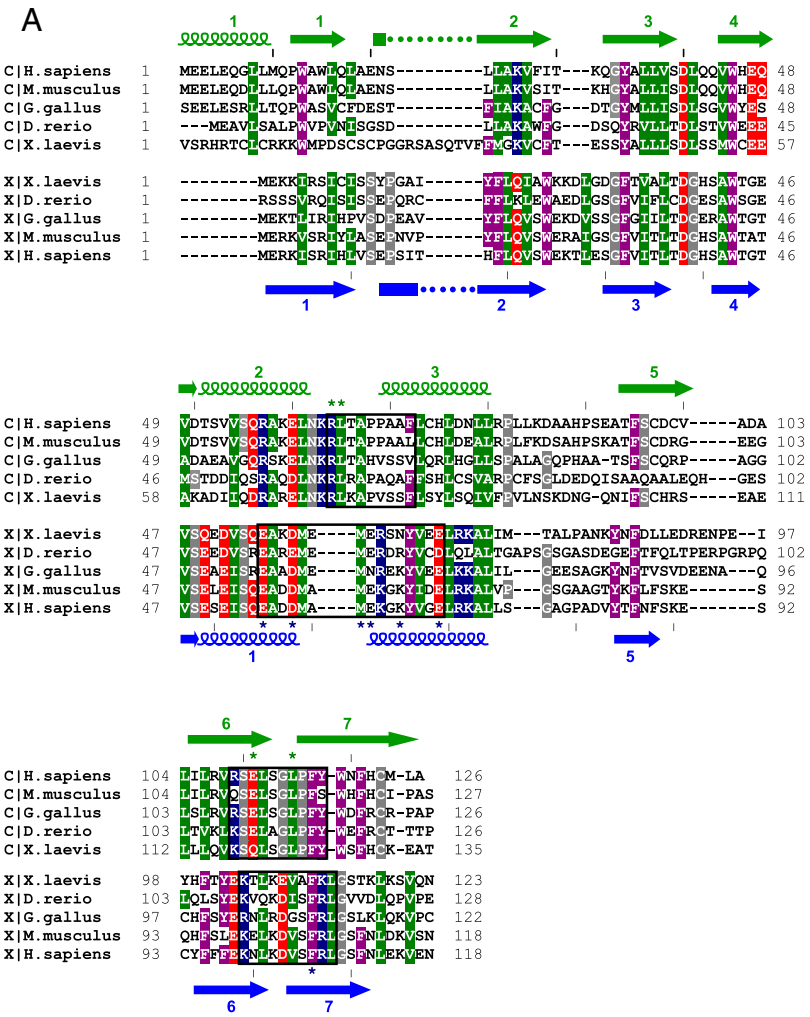
A
C|H.sapiens 1 MEELEQGLLMQPVAWLQLAENS---------LLAKVFIT---KQGYALLVSDLQQVWHEQ 48
C|M.musculus 1 MEELEQDLLLQPVAWLQLAENS---------LLAKVSIT---KHGYALLISDLQQVWHEQ 48
C|G.gallus 1 SEELESRLLTQPVASVCFDEST---------FIAKACFG---DTGYMLLISDLSGVWYES 48
C|D.rerio 1 ---MEAVLSALPVVPVNISGSD---------LLAKAWFG---DSQYRVLLTDLSTVWEEE 45
C|X.laevis 1 VSRHRTCLCRKKVMPDSCSCPGGRSASQTVFFMGKVCFT---ESSYALLISDLSSMWCEE 57
X|X.laevis 1 --------MEKKIRSLCISSYPGAI------YPLQLAWKKDLGDGFTVAITDCHSAWTGE 46
X|D.rerio 1 --------RSSSVRQISISEEPQRC------FFLKLEWAEDLGSGFVIFCDCESAWSGE 46
X|G.gallus 1 --------MEKTLIRLHPVSDPEAV------YFLQVSWEKDVSSGFGIILTDCERAWTGT 46
X|M.musculus 1 --------MERKVSRLYLASEPNVP------YFLQVSWERALGSGFVITLTDCHSAWTAT 46
X|H.sapiens 1 --------MERKISRLHLVSEPSIT------HFLQVSWEKTLESGFVITLTDCHSAWTGT 46
C|H.sapiens 49 VDTSVVSQRAKELNKRLTAPPAAFLCHLDNLLRFLLKDAAHPSEATFSCDCV-----ADA 103
C|M.musculus 49 VDTSVVSQRAKELNKRLTAPPAALLCHLDEALRFLFKDSAHPSKATFSCDRG-----EEG 103
C|G.gallus 49 ADAEAVCQRSKELNKRLTAHVSSVLQRLHGLLSFALAGQPHAA-TSFSCQRP-----AGG 102
C|D.rerio 46 MSTDDIQSRAQDLNKRLRAPAQAFFSHLCSVARFCFSGLDEDQISAAQAALEQH---GES 102
C|X.laevis 58 AKADITQDRARELNKRLKAPVSSFLSYLSQIVFFVLNSKDNG-QNIFSCHRS-----EAE 111
X|X.laevis 47 VSQEDVSQEAKDVE----MERSNVVEELRKALIM---TALPANKYNFDLLEDRENPE--I 97
X|D.rerio 47 VSPEDVSREAREME----MERDRVVCDLQIALTGAPSGSGASDEGETTFQLTPERPGRPQ 102
X|G.gallus 47 VSPAEISREAADVE----MNREKVVEELKKALIL---GEESAGKYNFTVSVDEENA---Q 96
X|M.musculus 47 VSELEISQEADDVA----MEKGKVIDELRKALVE---GSGAAGTYKFLFSKE-------S 92
X|H.sapiens 47 VSESEISQEADDVA----MEKGKVVGELRKALLS---GAGPADVYTFNFSKE-------S 92
C|H.sapiens 104 LIIRVRSELSGLPFY-WNFHGM-LA 126
C|M.musculus 104 LIIRVQSELSGLPFS-WHFHGI-PAS 127
C|G.gallus 103 LSIRVRSELSGLPFY-WDFRGR-PAP 126
C|D.rerio 103 LTVKLKSELAGLPFY-WEFRGT-TTP 126
C|X.laevis 112 LLLQVKSQLSGLPFY-WSFHGK-EAT 135
X|X.laevis 98 YHFTYEKTLKEVAFKLGSTKLKSVQN 123
X|D.rerio 103 LQLSYEKVQKDISFRLGVVDLQPVPE 128
X|G.gallus 97 CHFSYERNLRDGSFRLGSLKLQKVPC 122
X|M.musculus 93 QHFSLEKELKDVSFRLGSFNLDKVSN 118
X|H.sapiens 93 CYFFEKNLKDVSFRLGSFNLEKVEN 118
B
Y118C
M59X
α2
β7
β6
R109C
M61X
P116C
E62X
α2
α3
K65X
E111C
E69X
K99X
L101X

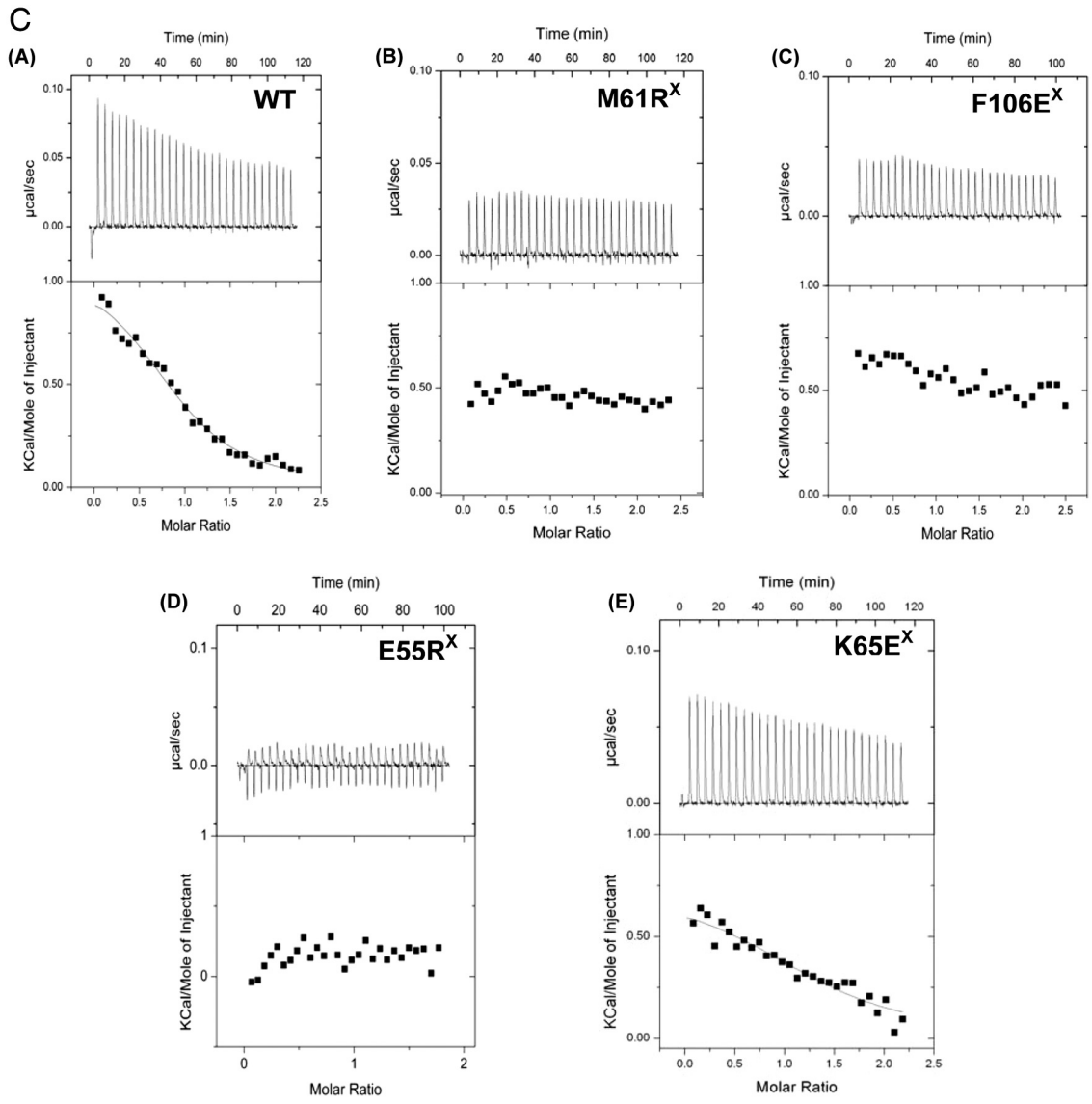
C
(A)
WT
(B)
M61R^X
(C)
F106E^X
(D)
E55R^X
(E)
K65E^X
Time (min)
µcal/sec
KCal/Mole of Injectant
Molar Ratio

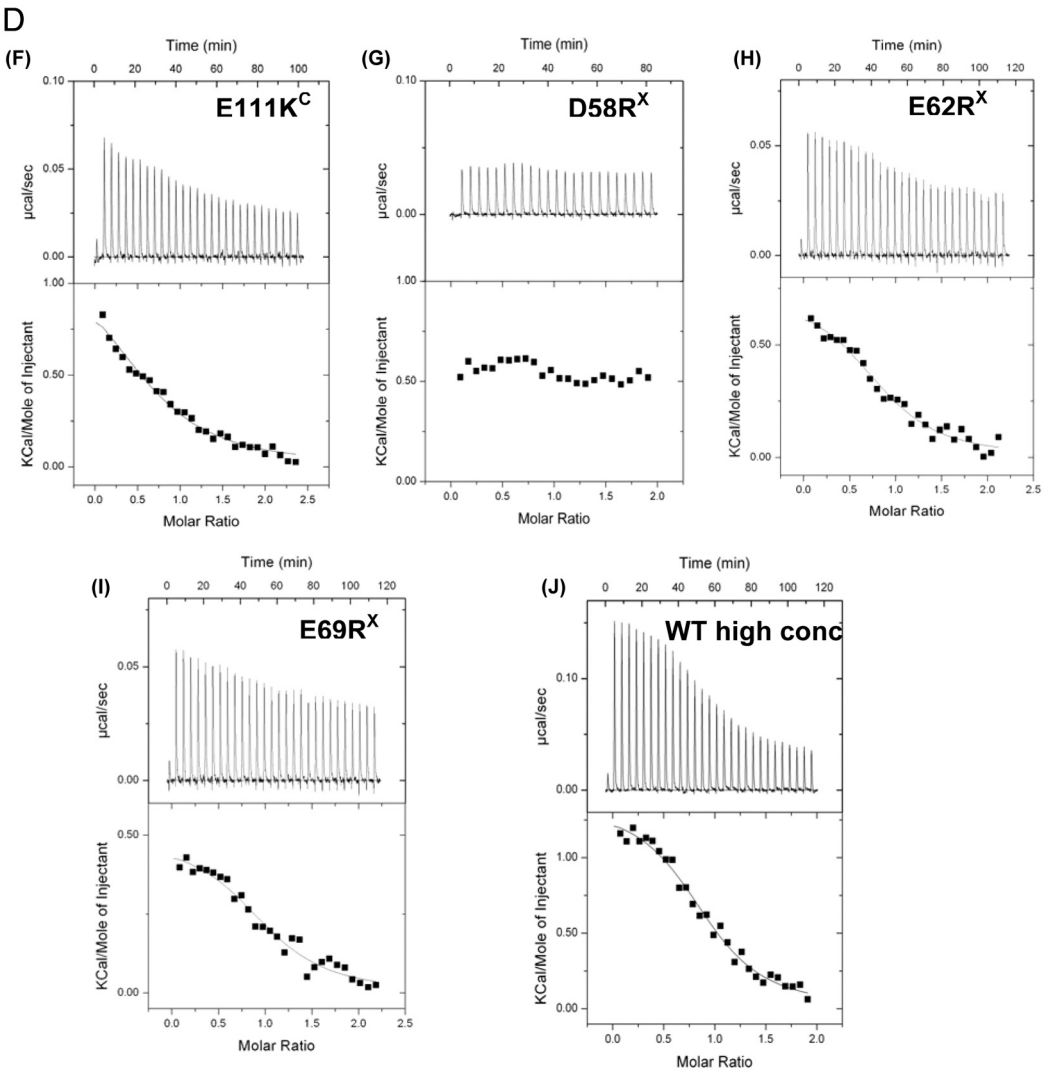

Fig. S3. (*A*) Structure-based sequence alignments of X4 and Cernunnos. Alignments of X4 and Cernunnos members were constructed on the basis of PSI-BLAST (1) and Muscle (2) results. The alignment between human X4 and Cernunnos was constructed from the 3D superimposition of the crystal structures of the proteins alone [for X4, PDB ID codes 1FU1 (3), 3II6 (4), 1IK9 (5), and for Cernunnos 2QM4 (6) and 2R9A (7)]. The secondary structures are indicated above and below, the Cernunnos ("C") and X4 ("X") sequences, respectively. Black rectangles indicate X4 and Cernunnos regions involved in the complex interface i1. The stars above and below, Cernunnos ("C") and X4 ("X") sequences, respectively, show the positions mutated by site-directed mutagenesis and analyzed by calorimetry. Alignments presented cover the head domains. Coloring scheme: white letters on a green background, positions in which hydrophobicity is conserved [on a purple background, conserved aromatic residues (F,W,Y)]; white letters on blue (K,R, H) or red (D,E) background for charged residues, white letters on a gray background, other noticeable conserved positions. (*B*) Second view of the X4–Cernunnos interface. The interface is rotated 180° along the horizontal axis compare to Fig. 3 in the main text. Color coding is the same, with X4 in cyan and Cernunnos in green. Dashed lines indicate inter- and intra-molecular hydrogen bonds and salt bridges between side-chain atoms proposed from Rosetta modeling. (*C*) Binding isotherms and integrated heats of Xrcc4 proteins (WT or variants) titrated by Cernunnos proteins (WT or variants). Upper panels show the binding isotherms. Lower panels show integrated heats, after subtraction of heats from control experiments. The black lines represent least-square fits of data. ITC binding isotherm obtained with WT Cernunnos and (**A**) X4 WT, (**B**) X4-M61R, (**C**) X4-F106E, (**D**) X4-E55R, and (**E**) X4-K65E. In these experiments, X4 at 20 μM is titrated by Cernunnos at 200 μM. Proteins are dialized against 25 mM sodium phosphate pH 8.0, 150 mM NaCl and 10 mM β-mercaptoethanol. The X4 K65E variant presents an intermediate profile with no saturation plateau. The fit of the data to a single-site interaction model does not allow to extract a Kd but simulations suggest at least a 10-fold decrease. (*D*) Binding isotherms and integrated heats of Xrcc4 proteins (WT or variants) titrated by Cernunnos proteins (WT or variants). ITC binding isotherms obtained with (**F**) Cernunnos-E111K and WT X4, (**G**) Cernunnos WT and X4-D58R, (**H**) Cernunnos WT and X4-E62R, (**I**) Cernunnos WT and X4-E69R (**J**) ITC binding isotherm obtained with proteins at 1.6 fold-higher concentration than in *A* and dialized against buffer with lower salt concentration (25 mM sodium phosphate pH 8.0, 75 mM NaCl and 10 mM betamercaptoethanol). The isotherm **J** with higher protein concentrations confirms the enthalpic and entropic values of the interaction between wild-type $X4^{1–157}$ and $Cernunnos^{1–224}$ proteins. The resulting thermograms produced a Kd of 4.6 ± 0.3 μM, which was similar to the Kd obtained with the lower protein concentrations (Kd of 4.1 ± 0.2 μM). These experiments allowed the enthalpy and entropy values of the interaction to be determined with higher precision. The interaction presents a small positive (unfavorable) enthalpy of +1.3 kcal/mol and a large negative (favorable) entropy term of −8.2 kcal/mol. These thermodynamic values suggest that the interface between the proteins is small and involves hydrophobic residues, both of which agree well with the characteristics of the i1 interface between X4 and Cernunnos.

1 Altschul SF, et al. (1997) Gapped BLAST and PSI-BLAST: A new generation of protein database search programs. *Nucleic Acids Res* 25:3389–3402.
2 Edgar RC (2004) MUSCLE: Multiple sequence alignment with high accuracy and high throughput. *Nucleic Acids Res* 32:1792–1797.
3 Junop MS, et al. (2000) Crystal structure of the Xrcc4 DNA repair protein and implications for end joining. *EMBO J* 19:5962–5970.
4 Wu PY, et al. (2009) Structural and functional interaction between the human DNA repair proteins DNA Ligase IV and XRCC4. *Mol Cell Biol* 29:3163–3172.
5 Sibanda BL, et al. (2001) Crystal structure of an Xrcc4-DNA ligase IV complex. *Nat Struct Mol Biol* 8:1015–1019.
6 Li Y, et al. (2008) Crystal structure of human XLF/Cernunnos reveals unexpected differences from XRCC4 with implications for NHEJ. *EMBO J* 27:290–300.
7 Andres SN, Modesti M, Tsai CJ, Chu G, Junop MS (2007) Crystal structure of human XLF: A twist in nonhomologous DNA end-joining. *Mol Cell* 28:1093–1101.

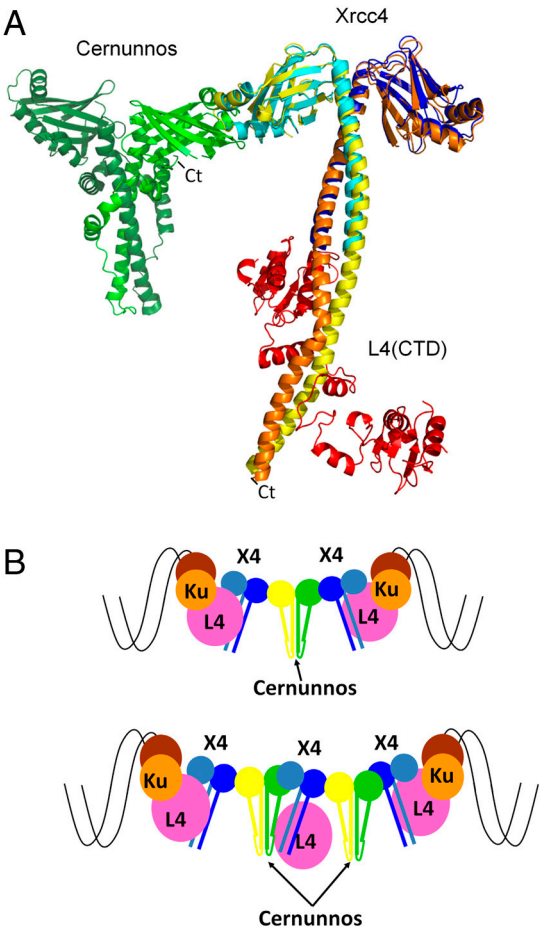

Fig. S4. (*A*) Superimposition of the structure of the complex between $X4^{1–203}$ and the C-terminal domain of $L4^{654–911}$ (L4-CTD) with the structure of the $X4^{1–157}$-Cernunnos$^{1–224}$ complex. We superimposed the X4 chain in contact with Cernunnos (in cyan) from our X4–Cernunnos complex structure with a X4 chain (yellow) from the X4-L4(CTD) (1) (PDB ID code 3II6). The two X4 chains superimposed well (rmsd = 1.2 Å over 600 atoms). The superimposition shows that the L4(CTD) (red) presents no steric hindrance with Cernunnos. The position of the C terminus of $X4^{1–203}$ and Cernunnos$^{1–224}$ are labeled "Ct" to indicate the direction of the C terminus regions of full-length $X4^{1–336}$ and Cernunnos$^{1–299}$ proteins. (*B*) Model of the stimulation of the final NHEJ ligation step by Cernunnos. The crystal structure of $X4^{1–157}$-Cernunnos$^{1–224}$ suggests that Cernunnos may facilitate the ligation step by bridging two *L4*/*X4* complexes bound to the two DSB extremities. The bridging could be mediated by one (model on top), two (model at the bottom) or more Cernunnos molecules consistent with the oligomer structures observed in vitro. This mechanism could help to adjust the positioning of *L4*/*X4* complexes according to the DSB geometry.

1 Wu PY, et al. (2009) Structural and functional interaction between the human DNA repair proteins DNA ligase IV and XRCC4. *Mol Cell Biol* 29:3163–3172.

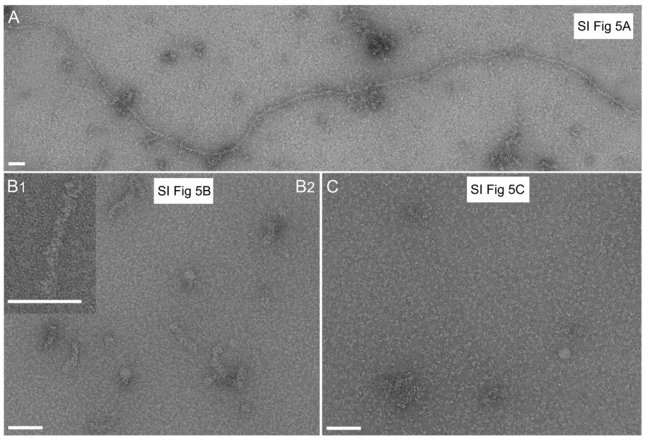
A
SI Fig 5A
B1
SI Fig 5B
B2
C
SI Fig 5C

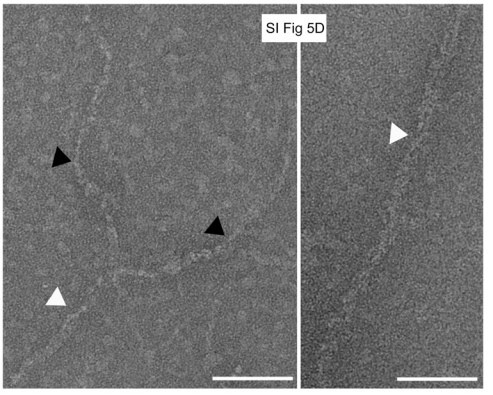
SI Fig 5D

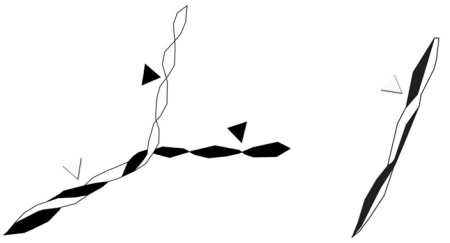

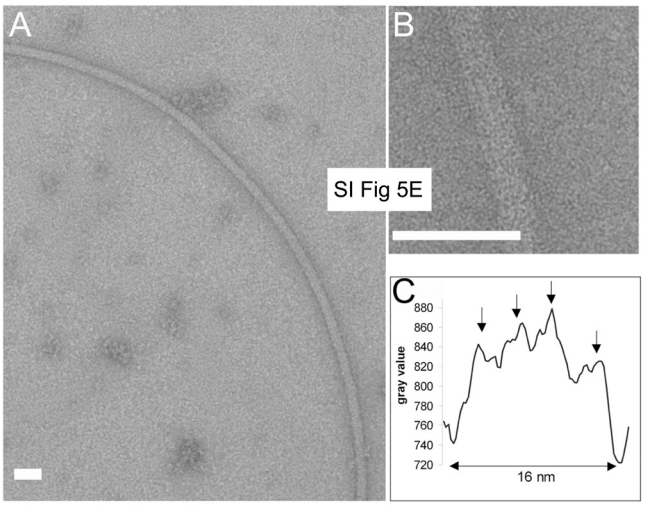
A
B
SI Fig 5E
C
880
860
840
820
800
780
760
740
720
gray value
16 nm

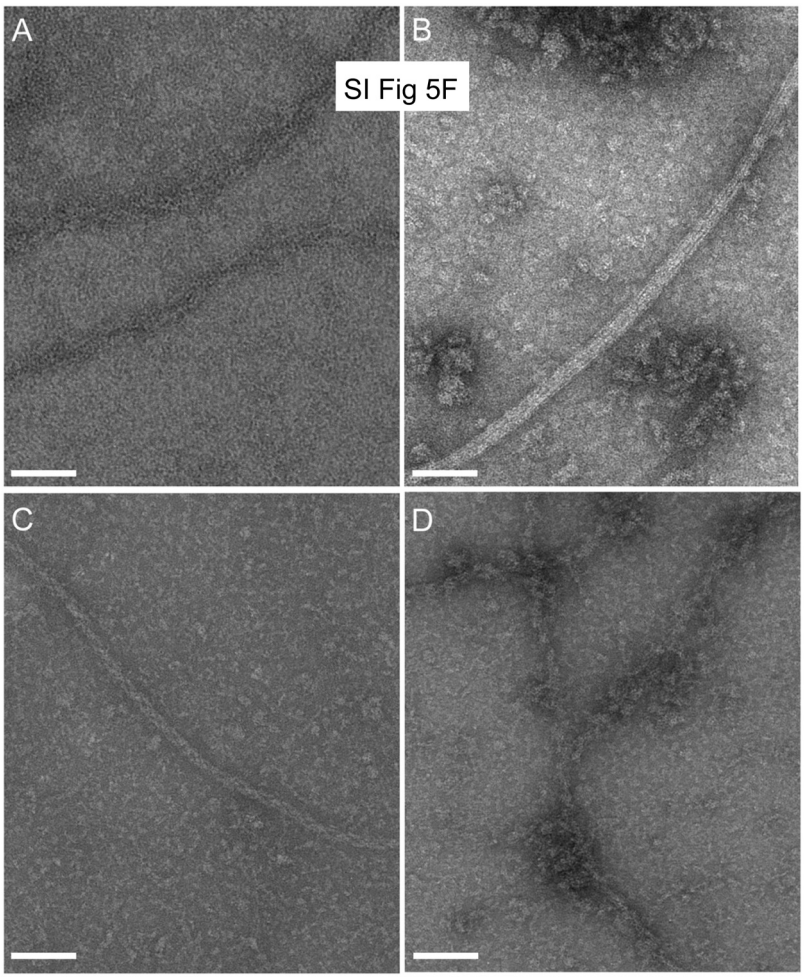

Fig. S5. (*A*) A long and typical filament of the Xrcc4–Cernunnos complex (2.5 μm) (magnification 13,860×). Bars in *A*–*F* represent 50 nm. (*B*) Short filaments (approximately 50 nm) of X4 protein (magnification b1: 63,000×, b2: 28,890×). (*C*) Cernunnos alone present no filaments. Some globular aggregates are observed on the grid (magnification 28,890×). (*D*) Micrographs and schematic models of 10-nm filaments constituted of two 5-nm filaments (micrographs are the same as Fig. 2 *B* and *C* in the main text). On the schematic model, the 5-nm filaments are represented in black and white. The black arrows on micrographs show the characteristic thinnest regions of 5-nm filaments that likely correspond to the rotation of the filament on itself. The heterogenous diameters of the 5-nm filaments are in agreement with the overall features of X4 and Cernunnos structures with protuding coiled-coil tail and globular N-terminal domain. (*E*) Electron micrographs of 20-nm large filaments of the X4–Cernunnos complex: (**a**) The approximately 20-nm filaments coexist with filaments of approximately 10 nm. These superstructures observed in electron micrographs are more regular and homogenous than the 10-nm filaments but remain curvilinear. They are fewer than the 10-nm filaments (approximately 10%). Their thickness ranges from 16 to 20 nm (magnification x 28980). (**b**) The magnification shows that the superstructure is composed of four filaments (magnification 63,000×). (**c**) For example, the gray level profile shows that the filament has a thickness of 16 nm and is composed of four regular thin filaments (black arrows). (*F*) Electron micrographs obtained with the X4 and Cernunnos full-length proteins. (**a**) Long and typical filaments observed with Xrcc4 full-length ($X4^{FL}$) protein alone. They resemble loosed braids. (**b**) $Cernunnos^{FL}$ makes essentially no filaments or some rare regular filaments as presented (straight and thickness of 20–25 nm). (**c** and **d**) Filaments observed with the $X4^{FL}$/$Cernunnos^{FL}$ complex. The filaments coexist with small aggregates of one, two, or more proteins (see **d**). The Xrcc4/Cernunnos filaments are present in large numbers; there are many long filaments 20–25 nm thick (**c**). Often two or more filaments combine like large ribbons. The 20–25-nm filaments resemble very tight braids (**c**) different from those observed with $X4^{FL}$ alone (**a**). Aggregates of Cernunnos appear to interact with the Xrcc4/Cernunnos filaments (**d**).

Table S1. Data collection and refinement statistics

Crystal		Wild Type	SeMet substituted
X-ray diffraction data			
Wavelength (Å)		1.044	0.97918
Spacegroup		$P6_522$	$P6_422$
Unit cell parameters:	a. b, c (Å)	103.91-103.91-856.73	105.08-105.08-427.47
	α, β, γ (deg)	90°-90°-120°	90°-90°-120°
Resolution range (Å)		58.9-5.5 (5.64-5.5)	39.83-6.6 (7.0-6.6)
Rsym (%) *		16.2 (144.8)	10.9 (136.0)
Completeness (%) *		85.4 (66.9)	99.5 (98.0)
Redundancy		20.4	11.3
No. of reflections		8 480	4 973
$\langle I/\sigma \rangle$ *		13.3 (2.0)	18.7 (2.4)
Mosaicity (deg)		0.15	0.18
			anomalous correlation† 62%SigAno: 1.57
Refinement and model quality			
Resolution range (Å)‡		56.9-5.0	
No. of reflections		13 059	
R-value (%)		26.6	
R-free (%)		31.5	
Overall mean B-factor (Å²)		252	
rmsd in bonds (Å)		0.009	
rmsd in angles (deg)		1.09	

*Highest resolution shell is shown in parentheses.

†Anomalous correlation is the correlation coefficient between signed anomalous differences: $|F_{hkl}| - |F_{-h-k-l}|$ as calculated by the XDS program (1).

‡Refinement was realized in resolution range 56.9 Å to 5.0 Å to use the information contained in reflections measured between 5.5 Å and 5.0 Å.

1 Kabsch W (2010) Integration, scaling, space-group assignment and post-refinement. *Acta Crystallogr D Biol Crystallogr* 66:133–144.